Geometrical optimization of a local ballistic magnetic sensor

Yuhsuke Kanda, Tatsuya Nomura, Takashi Kimura, and Masahiro Hara

Citation: Applied Physics Letters **104**, 142408 (2014); doi: 10.1063/1.4871002
View online: http://dx.doi.org/10.1063/1.4871002
View Table of Contents: http://scitation.aip.org/content/aip/journal/apl/104/14?ver=pdfcov
Published by the AIP Publishing

Geometrical optimization of a local ballistic magnetic sensor

Yuhsuke Kanda,[1] Tatsuya Nomura,[2] Takashi Kimura,[2,3] and Masahiro Hara[1]
[1]*Graduate School of Science and Technology, Kumamoto University, 2-39-1 Kurokami, Kumamoto 860-8555, Japan*
[2]*Advanced Electronics Research Division, INAMORI Frontier Research Center, Kyushu University, 744 Motooka, Fukuoka 819-0395, Japan*
[3]*Department of Physics, Kyushu University, 6-10-1 Hakozaki, Fukuoka 812-8581, Japan*

(Received 13 February 2014; accepted 30 March 2014; published online 9 April 2014)

We have developed a highly sensitive local magnetic sensor by using a ballistic transport property in a two-dimensional conductor. A semiclassical simulation reveals that the sensitivity increases when the geometry of the sensor and the spatial distribution of the local field are optimized. We have also experimentally demonstrated a clear observation of a magnetization process in a permalloy dot whose size is much smaller than the size of an optimized ballistic magnetic sensor fabricated from a GaAs/AlGaAs two-dimensional electron gas. © *2014 AIP Publishing LLC*. [http://dx.doi.org/10.1063/1.4871002]

Various types of magnetic nanoparticles are utilized not only in magnetic devices but also in medical diagnoses.[1–3] There are different types of biosensors for magnetic label detection: giant magnetoresistance (GMR) sensor,[1] Hall sensor,[4] anisotropic magnetoresistance (AMR) ring sensor,[5] spin-valve sensor,[6] and magnetoimpedance (MI) sensor.[7] A further miniaturization of the nanomagnets demands a highly sensitive local magnetic sensor for detecting a small amount of the magnetization. It is well known that a micro/nano superconducting quantum interference device (SQUID) sensitively detects a magnetic flux from an individual magnetic nanoparticle.[8–10] However, the SQUID sensors operate only below the critical temperature of the superconductor, which restricts fundamental analyses and applications in a wide range of temperatures including a room temperature. A sensitive detection based on anomalous Hall effect (AHE) reveals a magnetic behavior in a single nanodot with diameter range of several tens of nm.[11,12] Although a current flow inside the single ferromagnet is necessary for observing the AHE signal, typical nanoparticles are covered with insulating molecules for avoiding aggregations.[13] Hence, the AHE technique is applicable only for conductive magnetic nanoparticles with good electric contacts to the sensor.

As an alternative approach for the sensitive detection of a small magnet, we are focusing on the ballistic transports in two-dimensional electron systems. Ballistic trajectories of electrons in the sensor are deflected by the normal component of the local stray field from the magnet. The ballistic character effectively appears not in a Hall resistance but in a bend resistance. A contribution of the parallel component of the magnetic field is negligibly small so that we can detect a slight change in the magnetization under an external in-plane magnetic field. In fact, the magnetization reversal process of submicron-sized patterned ferromagnets were precisely investigated from ballistic bend resistance measurements using a micro-Hall cross in GaAs/AlGaAs two-dimensional electron gas (2DEG) systems.[14–17] We have also reported that the ballistic response with respect to an uniform magnetic field can be effectively tuned by changing the geometry of the sensor in recent.[18] In this Letter, we will report an approach for achieving higher sensitivity of the ballistic magnetometry for a nanomagnet by optimizing the sensor structure.

A schematic drawing of a 2DEG sensor with a permalloy (Py) dot, the target of the field detection in the present study, is shown in Fig. 1(a). The depth of the 2DEG plane from the surface in the magnetic sensor is 65 nm. In a two-dimensional conductor, the resistance dominantly depends on the magnetic field perpendicular to the conductive plane. When the permalloy dot is fully magnetized in the long axis (the $+x$ direction), stray fields from the both edges penetrate into the 2DEG plane as shown in Fig. 1(b). The estimated normal component of the stray field profile in the 2DEG plane is shown in Fig. 1(c). The amplitude of the magnetic

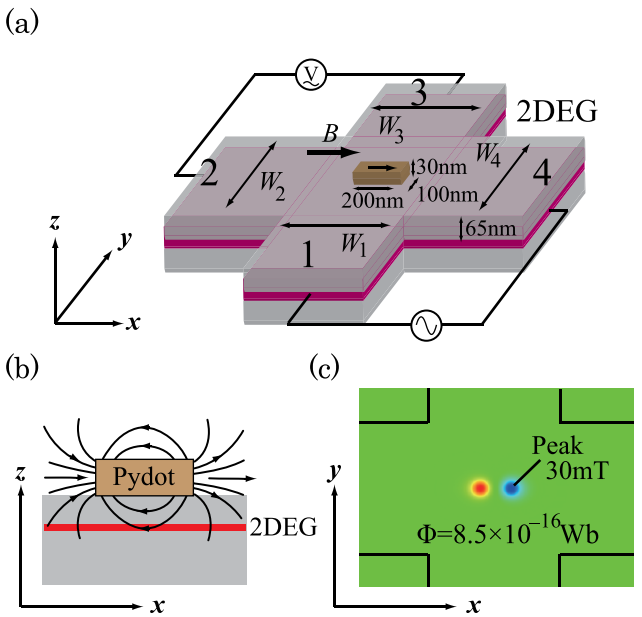

FIG. 1. (a) Geometry of the ballistic magnetic sensor with a Py dot. A bend resistance measured by the current-voltage configurations is sensitive to the local stray field from the Py dot. (b) Field profile of the stray field from the Py dot magnetized in the $+x$ direction. (c) Spatial distribution of the normal component of the stray field in plane of the 2DEG. The peak amplitude of the local field is about 30 mT.

flux from the each edge is about 8.5×10^{-16} Wb which is smaller than the flux quantum.

The transport properties in our 4-terminal mesoscopic conductor have been evaluated by numerical calculations based on the Landauer-Büttiker formula[19]

$$\frac{h}{2e} I_i = (N_i - T_{ii})\mu_i - \sum_{j \neq i} T_{ij}\mu_j. \quad (1)$$

Here, I_i, N_i, and μ_j are the current in lead i, the number of modes in lead i, and the chemical potential of lead j, respectively. T_{ij} describes the transmission probability of an electron injected from lead j to lead i.

We calculate the bend resistance $R_{14,23}$ with the probe configuration shown in Fig. 1(a). From the terminal conditions $I = I_1 = -I_4$; $I_2 = I_3 = 0$ for the bend-resistance measurement, the bend resistance R_B can be calculated as follows:

$$R_B = R_{14,23} = \frac{\mu_2 - \mu_3}{eI} = \frac{h}{2e^2} \frac{T_{34}T_{21} - T_{31}T_{24}}{D}, \quad (2)$$

where D is a factor independent of the current and voltage configuration.

In the simulation, we consider a 2DEG cross with 90° corners for simplicity. The electron density n_e and the Fermi wavelength λ_F in our sensor are assumed to be $3.8 \times 10^{15}/m^2$ and 41 nm, respectively. The channel width in lead i is defined as $W_i = N_i\lambda_F/2$. Electrons are injected from each probe like a billiard ball with an angular distribution $P(\alpha) = \cos\alpha/2$. Classical trajectories of electrons are modified by the estimated stray field from the Py dot. We then calculated transmission probabilities by counting number of the transmitted electrons into each probe.[20]

The calculated bend resistance depends on the geometry of the 2DEG cross. We consider the following three cases: (I) $N_1 = N_2 = N_3 = N_4 = N$, (II) $N_1 = N_3 = N$, $N_2 = N_4 = 90$, and (III) $N_1 = N_3 = 90$, $N_2 = N_4 = N$. Here, N is a variable parameter between 20 and 90 in the simulation. The Py dot magnetized in the $+x$ or the $-x$ direction is placed at the center of the sensor. Figure 2(a) shows the bend resistance as a function of channel number N in the type I. The bend resistance has a negative value, which is characteristic in ballistic conductors.[21] The absolute value of the resistance without the stray field from the Py dot $|R_B(0)|$ is proportional to the inverse of the channel number. The difference in the bend resistance between the positive magnetization R_B (+) and the negative magnetization R_B (−) is enhanced in smaller 2DEG cross. Figure 2(b) shows the bend resistance as a function of channel number N in the type II. The size-dependence of R_B (0) is relatively small comparing with the type I. The decrease of $N_1 = N_3$ value while keeping $N_2 = N_4$ constant leads to a significant difference between the positive and the negative magnetization $\Delta R = R_B(+) - R_B(-)$. By contrast, the decrease of $N_2 = N_4$ value (type III) leads to a much smaller difference. Figure 2(d) shows the relative sensitivity of the bend signal defined as $\Delta R/|R_B(0)|$ for the three cases. The type II is appropriate for a sensitive detection of stray fields from the tiny magnet.

In the above simulation, the target is placed at the center of the sensor. We also calculated the change in the bend resistance for shifting the position of the ferromagnet as shown in Fig. 3(a). The signal strongly depends on the position of the ferromagnet, which results from the ballistic transport property. The highest sensitivity is achieved when the ferromagnet is placed at the center of the type II sensor.

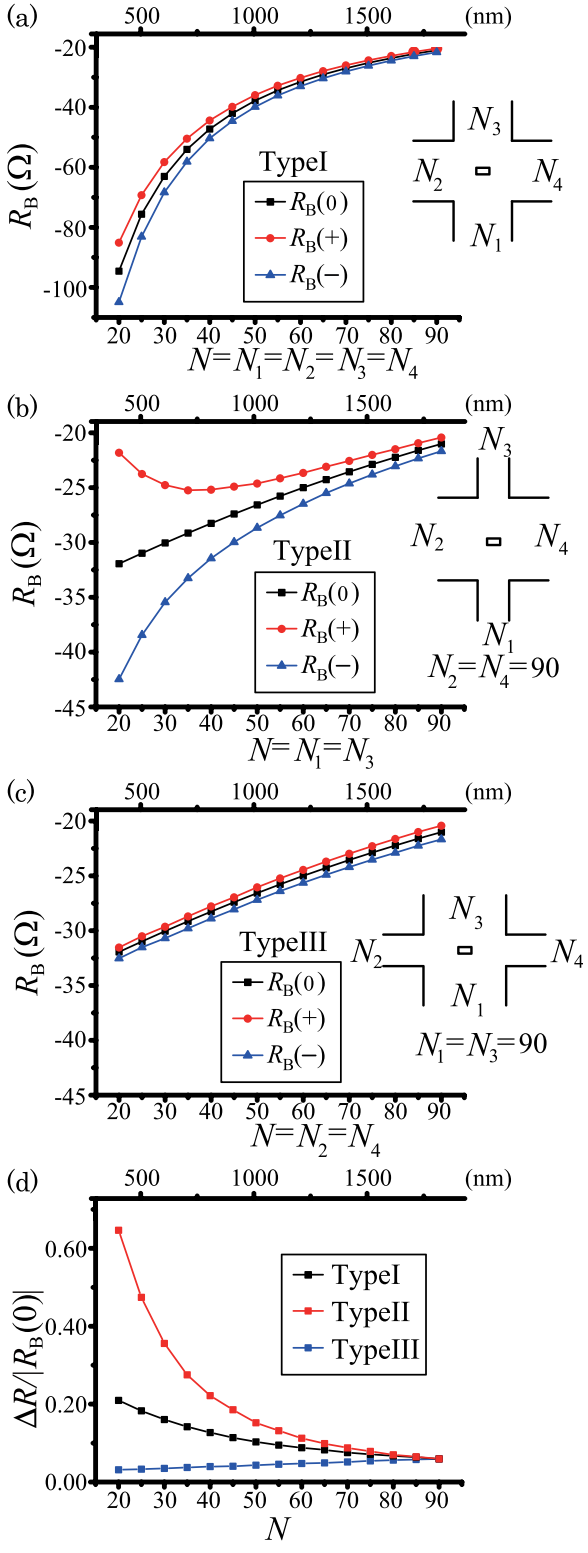

FIG. 2. Simulated bend resistance as a function of variable channel number N. (a) Type I: $N = N_1 = N_2 = N_3 = N_4$. (b) Type II: $N = N_1 = N_3 \leq N_2 = N_4 = 90$. (c) Type III: $N = N_2 = N_4 \leq N_1 = N_3 = 90$. (d) Relative sensitivity of the sensor as a function of channel number N for the three cases.

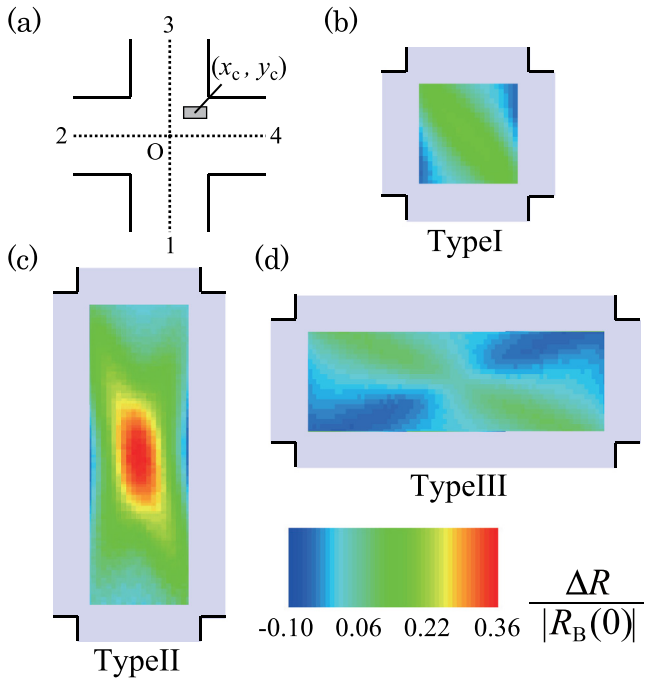

FIG. 3. (a) Schematic illustration of the position of the Py dot. The center of the Py dot (x_c, y_c) shifts from the origin. 2D mapping of the relative sensitivity of the ballistic sensor depending on the center of the Py dot for (b) type I, (c) type II, and (d) type III.

In order to demonstrate the high sensitivity in the type II sensor, we fabricated a sensor using a GaAs/AlGaAs 2DEG system. The density and mobility of the 2DEG before processing at 5 K were $3.8 \times 10^{15}/m^2$ and 68 m^2/V s, respectively. The depth of the 2DEG plane from the surface is 65 nm. The type II structure 0.6 μm × 1.8 μm was fabricated by means of Ar plasma etching. A scanning electron microscopy (SEM) image of the sample is shown in Fig. 4. The electron mean free path of the 2DEG is 6.9 μm at 5 K, which is larger than the size of the cross. A Py dot with thickness of 30 nm, width of 100 nm, and length of 200 nm is placed at the center of the sensor. The total magnetic moment of the Py dot is estimated to be 5×10^{-13} emu. 4-terminal resistance measurements were carried out using a low-frequency ac technique at 5 K.

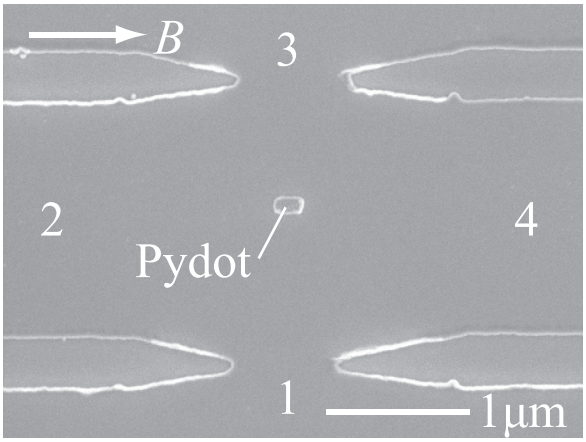

FIG. 4. SEM image of the fabricated sensor with a Py dot put on the center. The widths of the two terminal (1,3) is narrower than those of the other two terminals (2,4).

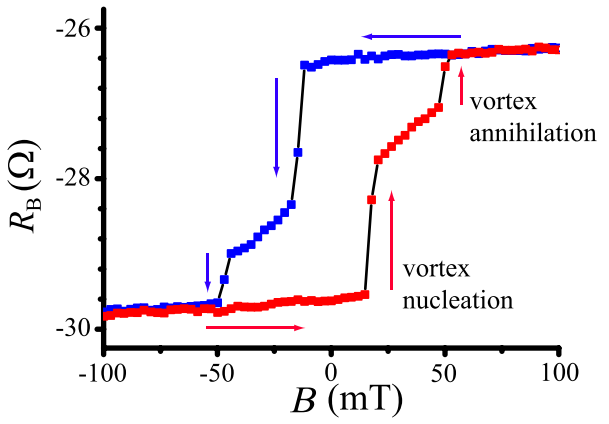

FIG. 5. Bend resistance $R_{14,23}$ as a function of in-plane magnetic field. A clear hysteresis curve was observed in the magnetization reversal process.

We measured a bend resistance $R_{14,23}$ as a function of in-plane magnetic field. We precisely aligned the magnetic field in the 2DEG plane so that the change in the resistance originates only from a stray magnetic field from the ferromagnet. As shown in Fig. 5, the change in the bend resistance reveals the magnetization reversal of the Py dot. The ballistic transport character in the optimized sensor enables us to detect a ferromagnet which is much smaller than the lateral size of the sensor. The observed two distinct resistance changes both in the forward and backward field sweeps implies that the magnetization reversal process proceeds through the nucleation and annihilation of the magnetic vortex.[22] Micromagnetic simulation using OOMMF[23] also supports that the Py dot with the same sample dimension favorably forms the vortex structure compared with the single domain structure. The relative sensitivity $\Delta R/|R_B(0)|$ is 0.13 in the experiment, which is smaller than the simulated value 0.36. The simulation overestimates the sensitivity since we assumes 90° corners of the junction and neglects any boundary and impurity scattering in the sensor.

In summary, we study a strategy for developing a highly sensitive ballistic magnetic sensor. A magnetization process of a Py dot was clearly observed in an optimized 2DEG sensor with two narrow terminals and two wide terminals when the Py dot was placed at the center of the sensor.

This work was supported by JSPS KAKENHI Grant Nos. 25870548 and 25220605.

[1]D. R. Baselt, G. U. Lee, M. Natesan, S. W. Metzger, P. E. Sheehan, and R. J. Colton, Biosens. Bioelectron. **13**, 731 (1998).
[2]D. L. Graham, H. A. Ferreira, and P. P. Freitas, Trends Biotechnol. **22**, 455 (2004).
[3]C. R. Tamanaha, S. P. Mulvaney, J. C. Rife, and L. J. Whitman, Biosens. Bioelectron. **24**, 1 (2008).
[4]P.-A. Besse, G. Boero, M. Demierre, V. Pott, and R. Popovic, Appl. Phys. Lett. **80**, 4199 (2002).
[5]M. M. Miller, G. A. Prinz, S.-F. Cheng, and S. Bounnak, Appl. Phys. Lett. **81**, 2211 (2002).
[6]D. L. Graham, H. Ferreira, J. Bernardo, P. P. Freitas, and J. M. S. Cabral, J. Appl. Phys. **91**, 7786 (2002).
[7]G. V. Kurlyandskaya, M. L. S'anchez, B. Hernando, V. M. Prida, P. Gorria, and M. Tejedor, Appl. Phys. Lett. **82**, 3053 (2003).
[8]M. Jamet, W. Wernsdorfer, C. Thirion, D. Mailly, V. Dupuis, P. Mélinon, and A. Pérez, Phys. Rev. Lett. **86**, 4676 (2001).

[9]L. Hao, C. Aβmann, J. C. Gallop, D. Cox, F. Ruede, O. Kazakova, P. Josephs-Franks, D. Drung, and Th. Schurig, Appl. Phys. Lett. **98**, 092504 (2011).
[10]R. Russo, C. Granata, E. Esposito, D. Peddis, C. Cannas, and A. Vettoliere, Appl. Phys. Lett. **101**, 122601 (2012).
[11]N. Kikuchi, S. Okamoto, O. Kitakami, Y. Shimada, and K. Fukamichi, Appl. Phys. Lett. **82**, 4313 (2003).
[12]A. Neumann, C. Thönniβen, A. Frauen, S. Heβe, A. Meyer, and H. P. Oepen, Nano Lett. **13**, 2199 (2013).
[13]H. Goesmann and C. Feldmann, Angew. Chem., Int. Ed. **49**, 1362 (2010).
[14]T. M. Hengstmann, D. Grundler, N. Klockmann, H. Rolff, Ch. Heyn, and D. Heitmann, IEEE Trans. Magn. **38**, 2535 (2002).
[15]M. Hara, J. Shibata, T. Kimura, and Y. Otani, Appl. Phys. Lett. **88**, 082501 (2006).
[16]M. Hara and Y. Otani, J. Appl. Phys. **101**, 056107 (2007).
[17]T. Matsunaga, K. Furukawa, Y. Kanda, M. Hara, T. Nomura, and T. Kimura, Appl. Phys. Lett. **102**, 252405 (2013).
[18]T. Matsunaga, M. Hidegara, K. Furukawa, M. Hara, T. Nomura, and T. Kimura, Appl. Phys. Express **5**, 073001 (2012).
[19]M. Büttiker, Phys. Rev. Lett. **57**, 1761 (1986).
[20]C. W. J. Beenakker and H. van Houten, Phys. Rev. Lett. **63**, 1857 (1989).
[21]Y. Takagaki, K. Gamo, S. Namba, S. Ishida, S. Takaoka, K. Murase, K. Ishibashi, and Y. Aoyagi, Solid State Commun. **68**, 1051 (1988).
[22]R. P. Cowburn, D. K. Koltsov, A. O. Adeyeye, M. E. Welland, and D. M. Tricker, Phys. Rev. Lett. **83**, 1042 (1999).
[23]M. Donahue and D. Porter, Interagency Report NISTIR 6376, National Institute of Standards and Technology, Gaithersburg, MD, 1999.